International Journal of Innovative Computing, Information and Control
Volume **21**, Number **3**, June **2025**

ICIC International ©2025 ISSN 1349-4198
pp. **633–648**

DYNAMIC EVALUATION OF ROCK MASS AND INFLUENCE OF SEED VALUES

Rui Huang[1,2], Takafumi Seiki[2], Qinxi Dong[3], Satoshi Yamaoka[2] and Ömer Aydan[4]

[1]School of Architecture and Civil Engineering
Xihua University
No. 999, Jinzhou Road, Jinniu District, Chengdu 610039, P. R. China
huangrui@mail.xhu.edu.cn

[2]School of Regional Development and Creativity
Utsunomiya University
7-1-2 Yoto, Utsunomiya City, Tochigi 321-8585, Japan
{ tseiki; yamaokast }@cc.utsunomiya-u.ac.jp

[3]School of Civil Engineering and Architecture
Hainan University
No. 58, Renmin Avenue, Haikou 570228, P. R. China
dongqinxi@hainanu.edu.cn

[4]University of the Ryukyus
1 Senbaru, Nishihara-cho, Nakagami-gun, Okinawa 903-0213, Japan
aydan@tec.u-ryukyu.ac.jp

Received October 2024; revised January 2025

Abstract. *The accurate assessment of rock mechanical parameters, which is crucial in the evaluation of rock mass quality and the selection of engineering design parameters, plays a significant role in the stability analysis of projects, as well as in the prediction, prevention, and control of disasters. Currently, there are numerous methods for identifying the mechanical parameters of rock masses, but few consider the impact of Rayleigh damping on the dynamic response of rock structures. Therefore, this study focuses on the identification of rock mass elastic moduli while considering Rayleigh damping. The proposed algorithm is based on the sensitivity analysis of the displacement response from the analytical model and employs truncated singular value decomposition. The time-varying sensitivity matrix is computed using numerical methods, and the effectiveness of the method is validated through a numerical study with an axisymmetric example subjected to impact excitation. The primary focus of our study is to discuss the influence of various factors included as the seed values on the inversion accuracy and convergence rate. The results indicate that the proposed inversion algorithm maintains stability even when seed values vary.*

Keywords: Inversion, Sensitivity, Damping, Seed values, Statistical analysis, Numerical simulation

1. **Introduction.** It is essential to estimate the mechanical parameters of rock mass for understanding and predicting their behavior in various engineering applications, such as rock mass strength, stability, and deformation characteristics of rock mass [1,2]. These mechanical parameters include Elastic Modulus (E), Poisson's Ratio, Angle of Internal Friction (Φ), Cohesion (C), etc., which are obtained through laboratory tests, field measurements, or numerical simulations. They constitute indispensable baseline data in

DOI: 10.24507/ijicic.21.03.633

geotechnical engineering design and construction. Damping significantly influences the dynamic response of rock mass, as it is a characteristic that reflects the dissipation of energy in materials or structures during vibration. It is crucial to consider the effects of damping in rock mechanics and engineering applications to accurately predict and assess the dynamic behavior of rock mass. Therefore, considering damping in rock mass parameter identification can facilitate more accurate modeling and forecasting of rock mass behavior under dynamic loading conditions. Despite a large amount of research, most of the research focuses on the identification of mechanical parameters of rock mass [3-5]. Rayleigh damping is rarely considered in the identification process, as achieving convergence may be difficult when including damping in the inversion analysis of rock mass parameters. The incorporation of damping parameters may increase the nonlinearity of the back calculation, making it more challenging to find the global optimal solution. Consequently, compared to elastic moduli and other parameters [6-8], it is difficult for existing methods to identify the damping coefficient of rock mass. Reasons for this include, but are not limited to, the proportionality of Rayleigh damping to the stiffness matrix, which increases linearly with frequency. Furthermore, Rayleigh damping requires compliance with specific orthogonality conditions in the finite element method (FEM), which may limit the accurate representation of the β coefficients.

The well-known concept of viscous damping, first introduced by Rayleigh [9], can be further simplified by a regular approach for selecting a damping matrix $\mathbf{C}$, which is achieved through the diagonalization of the classical normal modes. This form of damping, commonly referred to as classical damping, includes proportional damping, $\mathbf{C} = \alpha\mathbf{M}+\beta\mathbf{K}$, as a special case. Therefore, the selection of appropriate damping model and parameters is key to numerically simulating the dynamic response of rock mass. The damping ratio is the main index that reflects the dynamic characteristics of rock mass under earthquake and dynamic loading. Estimating the damping ratio usually involves experimental testing, theoretical analysis or numerical simulation.

It has been demonstrated that variations in the damping ratio can reflect the degree of material damage. When rock masses incur damage, the increase in internal cracks and micro-fractures leads to an increase in the damping ratio. Consequently, D'Angiò et al. [10] proposed a method for detecting rock mass damage by monitoring the temporal changes in the damping ratio associated with in-situ recorded vibrational events. The method may be more effective in environments subjected to periodic forcing. Under complex stress conditions, the failure process of rock mass is influenced by factors such as the amplitude of dynamic stress waves, the direction of perturbation, and the dip angle of structural planes. To reasonably describe the dynamic characteristics of rock mass, Yang et al. introduced an improved Hardin hyperbolic model to characterize the backbone curve of rock mass, establishing empirical formulas for estimating dynamic shear modulus and damping ratio [11]. However, the study was conducted based on specific rock types, such as granite and red sandstone, which may limit the universal applicability of the results. Moreover, experiments under laboratory conditions may not fully reproduce the complex stress states and dynamic disturbances encountered in actual underground engineering.

Consequently, this study employs the Rayleigh damping model and relies on engineering expertise to estimate the damping ratio. The seed values for the model parameters are determined by analyzing the lower-order vibration modes of the system. Additionally, the sensitivity of the acceleration response to the damping parameters is obtained using numerical methods such as time-stepping integration. The finite element analysis, displacement sensitivity analysis, and truncated singular value decomposition methods used in this research are also widely applied in other fields, as exemplified by the 3D FEM analysis of the fracture mechanism of hydroxyapatite under compressive load [12].

It has been observed that the selection of seed values significantly influences the solution of nonlinear optimization problems in the identification process of damping model coefficients and rock mass mechanical parameters. Cox and Teague [13] discussed methods based on layering ratios for identifying and incorporating the most reasonable stratified geologic models at a site in the absence of prior information, through systematic variation of identification parameterization, which can quantify the uncertainty of seed values. Researchers have also extensively applied global search methods such as Monte Carlo, genetic algorithms, and simulated annealing to exploring a broad parameter space, avoiding the issue of calculations becoming trapped in local minima due to initial model choices [14-17]. In the least squares method, the dependency on seed values is well recognized, highlighting the importance of selecting appropriate initial values for effective parameter estimation. However, it was found that the identification values of unknown parameters are independent of the seed parameters values in our work.

This study proposes a novel approach for the inversion estimation of elastic moduli and damping for rock mass. Subsequently, this study focuses on the selection range of seed values, different types of damping, and the number of measurement points, and discusses how these factors influence the inversion accuracy and convergence rate. The results indicate that even with changes in seed values, the proposed inversion algorithm can maintain stability.

2. Inversion Estimation of Elastic Moduli and Damping.

Although the stiffness coefficient β is a sensitive factor in the calculation process, numerical simulations suggest that relying solely on proportional damping based on stiffness is insufficient for accurately obtaining the results of back analysis [18]. In this research, we will determine the damping coefficients for the rock mass structure, assuming Rayleigh damping, by inverting computational simulation data.

2.1. Dynamic response analysis.

In dynamic finite element (FE) analysis, the equation of motion is given by [19]

$$\mathbf{M}\ddot{\mathbf{u}}(t) + \mathbf{C}\dot{\mathbf{u}}(t) + \mathbf{K}\mathbf{u}(t) = \mathbf{f}(t) \tag{1}$$

Here, $\mathbf{M}$, $\mathbf{C}$, and $\mathbf{K}$ represent the mass, damping, and stiffness matrices, respectively. The function $\mathbf{f}(t)$ represents the vector of loads that vary with time. The vectors $\ddot{\mathbf{u}}(t)$, $\dot{\mathbf{u}}(t)$ and $\mathbf{u}(t)$ correspond to acceleration, velocity, and displacement vectors, respectively. For rock mass simulations, Rayleigh damping is a prevalent and efficient approach. It is defined as a combination of the mass and stiffness matrices:

$$\mathbf{C} = \alpha\mathbf{M} + \beta\mathbf{K} \tag{2}$$

In this expression, α and β are coefficients that determine the proportionality to the mass and stiffness, respectively, which were established based on the damping ratio ξ and frequency characteristics of the rock mass structure, utilizing an eigenvalue analysis with initial estimates of the elastic moduli. For the general engineering structure, due to the dominant role of lower-order vibration modes in the dynamic response of the structure, the lower-order mode is usually used to determine the proportional coefficients α and β. Given the values of α and β, the damping ratios of other vibration modes can be determined using the formula, $\zeta_n = \frac{\alpha}{2\omega_n} + \frac{\beta\omega_n}{2} = \frac{1}{2}\left(\frac{\alpha}{\omega_n} + \beta\omega_n\right)$. Typically, two reference frequencies are chosen, and the values of α and β can be calculated based on the damping ratios at these two frequency points. Subsequently, the α and β were subjected to automatic adjustments within the program throughout the iterative process.

2.2. **Inversion estimation algorithm in time domain.** The difference between the measured and the numerically calculated displacement-time histories of rock mass at observation points can be used to evaluate an objective function within the framework of non-linear least-squares in the time domain. In general, an algorithm employs the trial values for the unknown parameters as input, refining them iteratively until the system model's response closely matches the measurements.

$$J(\mathbf{P}) = \frac{1}{2}\int_0^t \sum_{i=1}^{n} \left\{u_i(\mathbf{P},t) - u_i^*(t)\right\}^2 dt \tag{3}$$

Equation (3) involves n measurement points on the bedrock surface, where $u_i(\mathbf{P},t)$ and $u_i^*(t)$ represent the calculated and measured displacement-time histories, respectively. The unknown material parameters, contained in the vector $\mathbf{P} = (E_1, E_2, \ldots, E_m, \alpha, \beta)^T$, are optimized using iterative methods such as Newton, Quasi-Newton, and Gauss-Newton methods [20-24], where m represents the number of divided material domains within the rock mass.

These method iteratively update the parameters, starting with initial values, by solving Equation (3) until the solution converges to a local optimum. Specifically, the Gauss-Newton algorithm generates a sequence of parameters aimed at minimizing the objective function.

$$\mathbf{P}^{k+1} = \mathbf{P}^k + d\mathbf{P}^k \tag{4}$$

with

$$\mathbf{A}^k d\mathbf{P}^k = \mathbf{b}^k \tag{5}$$

where $\mathbf{A}^k$ equals $\int_0^t \left[J_P\left(\mathbf{P}^k\right)\right]^T \left[J_P\left(\mathbf{P}^k\right)\right] dt$; $\mathbf{b}^k$ equals $\int_0^t \left[J_P\left(\mathbf{P}^k\right)\right]^T \left[u_i\left(\mathbf{P}^k,t\right) - u_i^*(t)\right] dt$; J_P is the Jacobian matrix of displacement with respect to P; $d\mathbf{P}^k$ is increment vector.

The elements of the Jacobian matrix are represented by the sensitivity coefficients,

$$J_P = \begin{bmatrix} \dfrac{\partial u_1}{\partial E_1} & \dfrac{\partial u_1}{\partial E_2} & \cdots & \dfrac{\partial u_1}{\partial E_m} & \dfrac{\partial u_1}{\partial \alpha} & \dfrac{\partial u_1}{\partial \beta} \\ \dfrac{\partial u_2}{\partial E_1} & \dfrac{\partial u_2}{\partial E_2} & \cdots & \dfrac{\partial u_2}{\partial E_m} & \dfrac{\partial u_2}{\partial \alpha} & \dfrac{\partial u_2}{\partial \beta} \\ \vdots & \vdots & \vdots & \vdots & \vdots & \vdots \\ \dfrac{\partial u_n}{\partial E_1} & \dfrac{\partial u_n}{\partial E_2} & \cdots & \dfrac{\partial u_n}{\partial E_m} & \dfrac{\partial u_n}{\partial \alpha} & \dfrac{\partial u_n}{\partial \beta} \end{bmatrix} \tag{6}$$

In solving the parameter inversion extimation problems, an efficient and convenient method must be adopted in the calculation of the sensitivity coefficient.

Based on J_P, $\mathbf{A}^k$ is an $(m+2)\times(m+2)$ matrix of displacement sensitivity coefficients, $\mathbf{b}^k$ is an $(m+2)\times 1$ vector of error values, and $d\mathbf{P}^k$ is the increment of the unknown parameter vector.

$$\begin{aligned} \mathbf{A}_{jl}^k &= \int_0^t \left(\sum_{i=1}^{n} \frac{\partial u_i}{\partial p_j}\frac{\partial u_i}{\partial p_l}\right) dt \\ \mathbf{b}_j^k &= \int_0^t \left(\sum_{i=1}^{n} \left\{\left(u_i\left(\mathbf{P},t\right) - u_i^*(t)\right)\frac{\partial u_i}{\partial p_j}\right\}\right) dt, \quad (j,l = 1,2,\ldots,m+2) \\ d\mathbf{P}^k &= \left\{dp_1^k, dp_2^k, \ldots, dp_{m+2}^k\right\}^T \end{aligned} \tag{7}$$

2.3. **Sensitivity analysis in the time domain.** Given that the loading is independent of material properties, and the system's mass is separate from material parameters, it is

solely the stiffness matrix that is associated with the material parameters. By differentiating both sides of Equation (1) with respect to the material-specific parameters E_j, α and β, the following is derived:

$$\mathbf{M}\frac{\partial \ddot{\mathbf{u}}}{\partial E_j} + (\alpha\mathbf{M} + \beta\mathbf{K})\frac{\partial \dot{\mathbf{u}}}{\partial E_j} + \mathbf{K}\frac{\partial \mathbf{u}}{\partial E_j} = -(\mathbf{u} + \beta\dot{\mathbf{u}})\frac{\partial \mathbf{K}}{\partial E_j} \tag{8}$$

$$\mathbf{M}\frac{\partial \ddot{\mathbf{u}}}{\partial \alpha} + (\alpha\mathbf{M} + \beta\mathbf{K})\frac{\partial \dot{\mathbf{u}}}{\partial \alpha} + \mathbf{K}\frac{\partial \mathbf{u}}{\partial \alpha} = -\mathbf{M}\dot{\mathbf{u}} \tag{9}$$

$$\mathbf{M}\frac{\partial \ddot{\mathbf{u}}}{\partial \beta} + (\alpha\mathbf{M} + \beta\mathbf{K})\frac{\partial \dot{\mathbf{u}}}{\partial \beta} + \mathbf{K}\frac{\partial \mathbf{u}}{\partial \beta} = -\mathbf{K}\dot{\mathbf{u}} \tag{10}$$

where E_j, α and β are the unknown parameters, and the right-hand sides represent the pseudo-force vectors. The sensitivity $\partial\ddot{\mathbf{u}}/\partial p_j$, $\partial\dot{\mathbf{u}}/\partial p_j$ and $\partial\mathbf{u}/\partial p_j$ with respect to the elastic moduli and Rayleigh damping coefficients can then be solved using the Newmark-β method for step-by-step time integration from Equations (8) to (10). Once displacement sensitivity $\partial\mathbf{u}/\partial p_j$ is calculated, then sensitivity matrix $\mathbf{A}$ and right-hand side vector $\mathbf{b}$ described in Equation (5) are generated.

The parameter inversion estimation procedure, as shown in Figure 1, can be expressed as follows.

Step 1: The angular frequency ω can be obtained from eigenanalysis. Set the angular frequencies ω_m and ω_n, and the initial α_0, β_0 and the sensitivity matrix $\partial\mathbf{K}/\partial\mathbf{P}$ can be calculated.

Step 2: Computing stiffness matrix $\mathbf{K}$, solve Equation (1), and Equations (8) to (10) for $k = 1$.

Step 3: Solve Equation (5) to get the unknown parameter $d\mathbf{P}^k$, and update $\mathbf{P}^{k+1} = \mathbf{P}^k + d\mathbf{P}^k$.

Step 4: The total number of iteration k is determined when the following convergence criteria are met: $\left|dp_j^k/p_j^k\right| < \varepsilon = 10^{-3}$, $j = 1, \ldots, m+2$. If the criterion is met, the iterative process stops. Otherwise, set $k = k + 1$ and return to Step 2, repeating until convergence is achieved.

3. **Numerical Simulation Study.**

3.1. **A multi-layered rock mass structure.**

Assuming a multi-layered structure for rock mass in numerical analysis is a prevalent method, highly effective for simulating and analyzing the physical behavior of rock masses.

An axisymmetric finite element model with a 20 m × 20 m, consisting of 441 8-node solid elements and 1408 nodes, is shown in Figure 2(a). The minimum mesh size is 0.0095 m. The five red dots in Figure 2, designated as A, B, C, D, and E, respect to the five accelerometers laid out horizontally in the same direction. Their respective distances from the 5.5 kN weight with excitation point are 0.3 m, 0.6 m, 1.2 m, 2.4 m, and 4.8 m. Acceleration responses at point A in the x-, y- and z-directions were recorded, but only the z-direction acceleration response was used to obtain displacement-time histories as input data. This response is believed to contain more of the strain energy in the structure's vibration motion. We assume that the first and second layers of rock mass are loose- and flesh-colored, respectively. The initial value of elastic moduli for the first and second layers as $E_1 = 7.36$ GPa and $E_2 = 8.08$ GPa, respectively, based on previous experimental data and literature reviews that suggest these values are representative of the materials used. The Poisson's ratio was chosen to be 0.23, which is a typical value for isotropic materials within the elastic range. The density of 1770 kg/m^3 was selected to match the

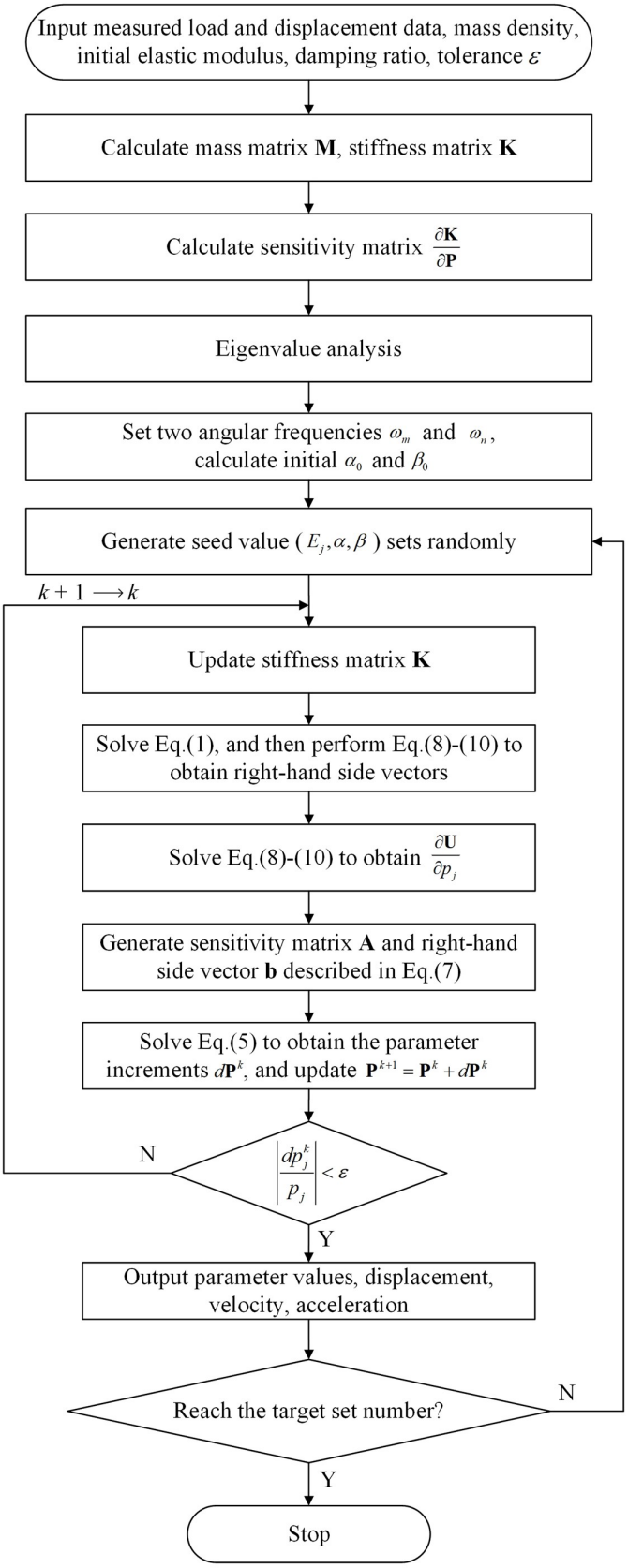

FIGURE 1. Flow chart of parameter inversion estimation procedure

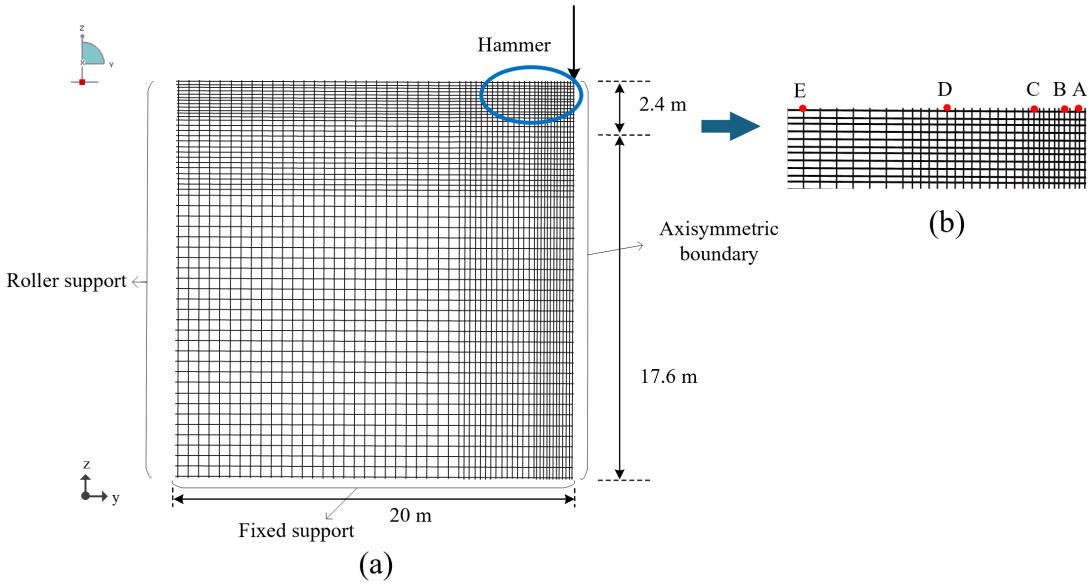

FIGURE 2. The in-site of the shock vibration experiment with layered media of the simulated rock mass: (a) FE mesh; (b) the location of the accelerometers

known density of the material in question, ensuring that the mass properties used in the simulation align with real-world characteristics.

3.2. **Accuracy of dynamic forward analysis.** The natural angular frequency ω and fundamental frequency f of the structure were determined via eigenvalue analysis. With an assumed damping ratio ξ of 3%, two angular frequencies were arbitrarily selected to verify the optimality of different combinations. The damping coefficients α and β were calculated using $\alpha = 2\omega_m\omega_n\xi/(\omega_m + \omega_n)$ and $\beta = 2\xi/(\omega_m + \omega_n)$, representing the true values of the rock mass damping coefficients. In this work, the calculation of eigenvalues was extended to the 30th order, and five sets of angular frequencies were freely combined to obtain their respective true values of damping coefficients, as shown in Table 1.

TABLE 1. True values of damping coefficients for different combinations

	α_0 (1/s)	β_0 (s)	Note
case 1	6.3311	1.3867×10^{-4}	1st and 2nd order
case 2	9.3568	4.7783×10^{-5}	1st and 30th order
case 3	8.8284	6.3654×10^{-5}	1st and 15th order
case 4	32.075	2.8058×10^{-5}	29th and 30th order
case 5	26.698	3.2727×10^{-5}	15th and 30th order

The true values derived from these calculations are then input into the forward analysis to generate the displacement-time histories at the five observation points for each of the five groups of cases, as shown in Figure 3.

At observation point A, which exhibits the most significant variation, it is evident that the peak of the blue curve is delayed relative to the other curves, strongly suggesting that β is the predominant parameter influencing viscous damping. Given that the peak displacements and their corresponding elapsed times for the other groups are comparable to those at point A, it is justified that angular frequencies can be freely combined within

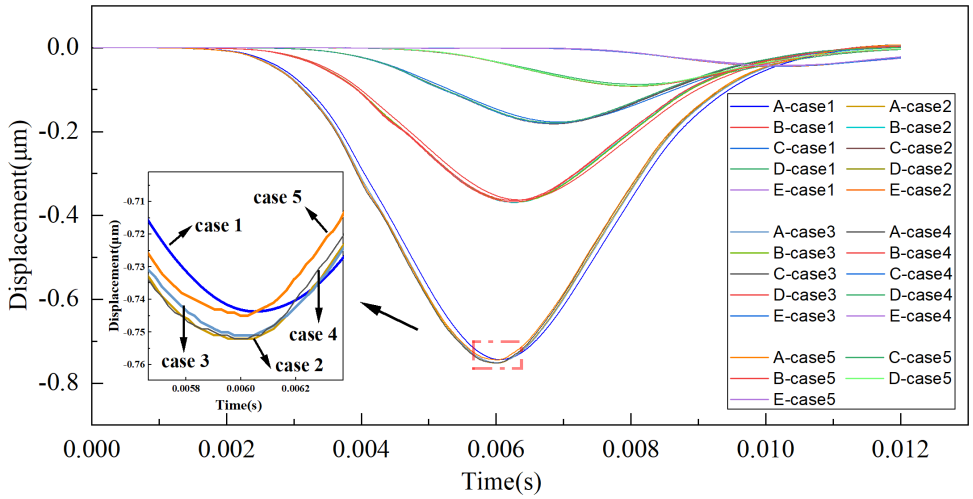

FIGURE 3. (color online) The displacement of 5 measurements points with different cases

our study. Subsequently, these combinations were individually compared against the observational data.

3.3. **Parameters inversion estimation.** The rock mass was subject to the vibration excitation in three directions as plotted in Figure 4. The damping model in Equation (2) was adopted with damping ratio ξ of 3% in the computation of the dynamic response for the parameters inversion estimation. In the iteration procedure, the initial values for elastic moduli and Rayleigh damping were assumed to be their true values. Elastic moduli and Rayleigh damping were identified simultaneously. The sampling frequency is 500 Hz and the responses recorded in 0.04 second are used for the identification of elastic moduli and Rayleigh damping with the parameter vector $\mathbf{P} = (E_1, E_2, \ldots, E_m, \alpha, \beta)^T$. The sensitivities of the $\partial\ddot{\mathbf{u}}/\partial p_j$, $\partial\dot{\mathbf{u}}/\partial p_j$ and $\partial\mathbf{u}/\partial p_j$ response in z-direction with respect to the elastic moduli and Rayleigh damping coefficients were computed using the Newmark-β method for step-by-step time integration.

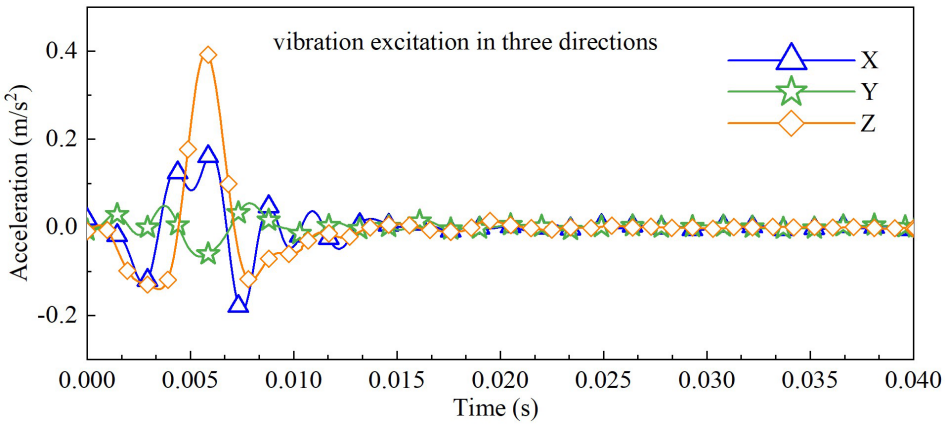

FIGURE 4. The vibration excitation in x-, y- and z-directions

3.4. **Effect of seed value.** The effect of different seed values on the identified results is also studied with the "measured" displacement response simulated from the analytical model. The study examines various seed values, including the range of seed values, damping coefficients, and the number of measurement points.

3.4.1. *Selection of seed values.* In-depth investigation of the influence of seed value selection on the inversion outcomes of rock mechanical parameters was conducted. A total of 4000 sets of initial values were randomly generated within the range spanning 50% to 150% of the true values. Each set was subjected to 1000 simulations for four parameters $(E_1, E_2, \alpha, \beta)$. The diversity and randomness of the seed values were ensured through the application of the Monte Carlo method, simulating the parameter uncertainty likely to be encountered in practical engineering applications.

To visually represent the distribution characteristics of these seed values, a scatter density plot was constructed as shown in Figure 5, which vividly illustrates the distribution of initial values within various intervals. It was found that the initial values were relatively evenly distributed across each interval, offering a rational basis for the subsequent inversion calculations.

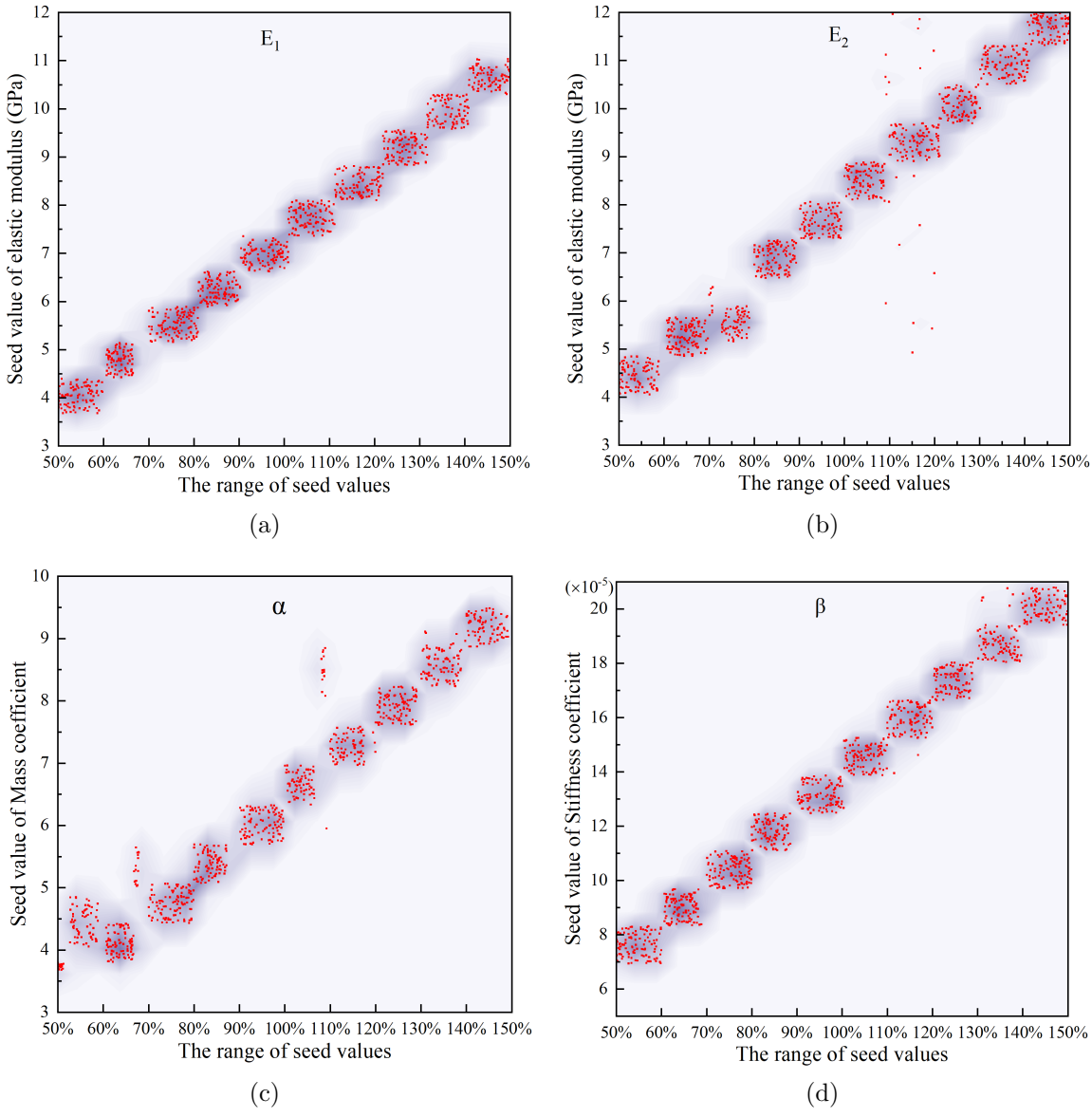

FIGURE 5. The range of seed values for back calculation: (a) Elastic modulus E_1, (b) elastic modulus E_2, (c) Rayleigh damping coefficient α, and (d) Rayleigh damping coefficient β

However, utilizing all 4000 sets of data for inversion calculations is impractical due to the immense computational resources and time consumption. To address this issue, a subset of initial values was selected, comprising 50%, 60%, 70%, ..., 150% of the true values, as well as the average values of the intervals between these percentages, resulting in a total of 21 representative sets. These were used to conduct inversion calculations to assess their impact on the inversion outcomes. The computational results are presented in Table 2.

TABLE 2. Inversion values with different seed values

Case	True value	E_1 (GPa)		E_2 (GPa)		α (1/s)		β (s)	
		Seed value	Inversion value	Seed value	Inversion value	Seed value	Inversion value	Seed value ($\times 10^{-5}$)	Inversion value ($\times 10^{-4}$)
1	50%	3.6800	6.0710	4.0400	8.1107	3.1656	3.1693	6.9335	1.1958
2	50% to 60% Avg.	4.0488	6.0723	4.4370	8.1064	3.7397	3.7434	7.6176	1.1943
3	60%	4.4160	6.0699	4.8480	8.1058	3.7987	3.8012	8.3202	1.1941
4	60% to 70% Avg.	4.7768	6.0715	5.2692	8.1037	4.0981	4.0999	8.9863	1.1933
5	70%	5.1520	6.0685	5.6560	8.1006	4.4318	4.4333	9.7069	1.1923
6	70% to 80% Avg.	5.5267	6.0725	6.0000	8.0989	4.7439	4.7350	1.0361	1.1916
7	80%	5.8880	6.0709	6.4640	8.0963	5.0649	5.0653	1.1093	1.1907
8	80% to 90% Avg.	6.2381	6.0748	6.8825	8.0931	5.3818	5.3742	1.1813	1.1897
9	90%	6.6240	6.0688	7.2720	8.0908	5.6989	5.6970	1.2480	1.1888
10	90% to 100% Avg.	6.9722	6.0748	7.6383	8.0873	6.0199	6.0143	1.3145	1.1877
11	100%	7.3600	6.0705	8.0800	8.0855	6.3311	6.3284	1.3867	1.1870
12	100% to 110% Avg.	7.7390	6.0684	8.6268	8.0832	6.6738	6.6751	1.4572	1.1861
13	110%	8.0960	6.0703	8.8880	8.0808	6.9642	6.9595	1.5253	1.1853
14	110% to 120% Avg.	8.4292	6.0671	9.3103	8.0786	7.2678	7.2704	1.5993	1.1845
15	120%	8.8320	6.0682	9.6960	8.0761	7.5973	7.5906	1.6640	1.1836
16	120% to 130% Avg.	9.1961	6.0669	10.0546	8.0737	7.9185	7.9110	1.7379	1.1827
17	130%	9.5680	6.0698	10.5040	8.0719	8.2304	8.2230	1.8027	1.1820
18	130% to 140% Avg.	9.9383	6.0686	10.9357	8.0695	8.5432	8.5376	1.8664	1.1812
19	140%	10.3040	6.0669	11.3120	8.0667	8.8635	8.8621	1.9413	1.1802
20	140% to 150% Avg.	10.6607	6.0686	11.7426	8.0643	9.1744	9.1536	9.8672	1.1794
21	150%	11.0400	6.0652	12.1200	8.0611	9.4967	9.5510	2.0800	1.1782

Subsequently, a statistical analysis was conducted on each set of inversion results. This analysis calculated the standard deviation and variance to quantify the dispersion of the inversion values. The results of this analysis are presented in Table 3.

TABLE 3. Statistical analysis of inverted rock mechanics parameters

Parameter	Mean (μ)	Standard deviation (Std)	Variance
E_1 (GPa)	6.0698	2.823×10^{-3}	6.348×10^{-6}
E_2 (GPa)	8.0846	2.512×10^{-2}	6.312×10^{-4}
α (1/s)	3.1693	1.941×10^{-3}	3.749×10^{-6}
β (s)	1.1958×10^{-4}	2.080×10^{-6}	4.384×10^{-10}

The results demonstrate that the standard deviations and variances of the inversed rock mechanics parameters (E_1, E_2, α, β) fall within acceptable ranges, indicating that the identification process possesses stability and independence, even when the seed values are subject to considerable variation.

To provide a visual representation of these outcomes, comparison graphs between the inversed values and the true values have been constructed as shown in Figure 6. The

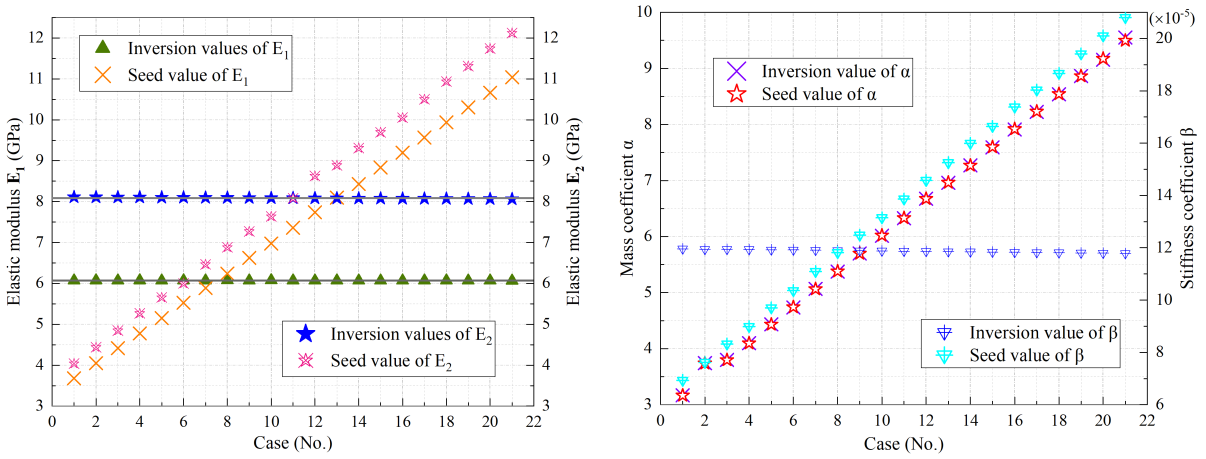

FIGURE 6. The identification results of 21 cases: (a) Elastic moduli; (b) Rayleigh damping coefficient

figure illustrates that the inversed values closely follow the true values, despite the seed values exhibiting substantial variation across a broad range, thereby further validating the stability and reliability of the inversion process.

3.4.2. *Damping coefficients.* Different scenarios involving damping coefficients in rock masses were investigated to understand their impact on the inversion process. Specifically, mass coefficients (α) and stiffness coefficients (β) were identified separately. The various damping identification scenarios are detailed in Table 4.

TABLE 4. Inversion value of different damping coefficients

Seed value	Elastic moduli (GPa)		Rayleigh damping		Iterations (No.)
	E_1	E_2	α (1/s)	β ($\times 10^{-4}$) (s)	
	7.36	8.08	6.3311	1.3867	
case 1	6.07	8.09	6.3311	1.1869	7
case 2	6.07	8.09	6.3311	1.1869	7
case 3	6.04	8.42	6.3362	1.1869	6

According to Table 4, Figure 7 is plotted, and it can be observed more intuitively that the required accuracy and iteration times for identifying four parameters simultaneously are almost the same as those for identifying only three parameters. This indicates that even when identifying parameters of different orders of magnitude simultaneously, the identification process can still converge rapidly. However, when β is fixed and only three parameters (E_1, E_2, α) are identified, as in the case 3 of Table 4, the inversion results for the elastic modulus E_2 are not as accurate as in case 1 (where both α and β are included in the inversion), which is consistent with the conclusion that β is sensitive in the identification process.

3.4.3. *The number of measurement points.* Different numbers with measurement points on the surface of rock mass are investigated. In the process of identifying rock mass material parameters, it is crucial to discuss the impact of the number of measurement points on the identification results, as the representativeness and coverage of the spatial variability of rock mass parameters are affected by the quantity of measurement points. An adequate

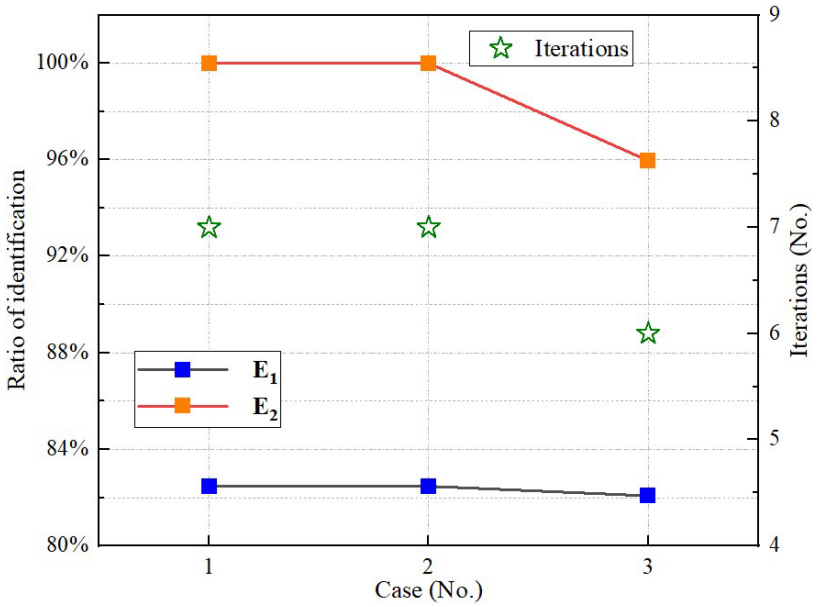

FIGURE 7. Inversion ratio and number of iterations with different cases

TABLE 5. Inversion values of different numbers of measurement points

Measurement point (No.)	Elastic moduli (GPa)		Rayleigh damping coefficient		Iterations (No.)
	E_1	E_2	α (1/s)	$\beta \times 10^{-4}$ (s)	
1	6.08	7.91	6.3312	1.1429	5
2	6.08	7.98	6.3294	1.1569	5
3	6.07	8.04	6.3283	1.1738	5
4	6.07	8.08	6.3285	1.1863	7
5	6.07	8.09	6.3311	1.1869	7

number of measurement points can more comprehensively reflect the heterogeneity of the rock mass, which may also affect the accuracy and stability of the algorithm, as some algorithms require a sufficient number of data points to ensure the convergence and accuracy of the solution [25]. Accordingly, the following discussion, detailed in Table 5, examines these effects.

The analysis from Figure 8 indicates that the identification results of the elastic moduli are independent of the number of observation points. The identification results for the Rayleigh damping coefficients show subtle changes, with a higher quantity of measurement data leading to greater accuracy in the identification results. This reaffirms the sensitivity of β in the back calculation process. However, the negligible differences in precision also demonstrate that the inversion method possesses considerable robustness, enabling stable parameter identification even with a limited measured data. This is also associated with the rock mass exhibiting a good degree of uniformity within the scope of investigation, without pronounced signs of heterogeneity or anisotropy.

4. **Discussions.** In comparison with other damping identification methods, the approach presented in this study exhibits a heightened tolerance to variations in seed values. It is capable of concurrently identifying the elastic moduli and Rayleigh damping of rock masses, addressing the challenges faced by conventional methods in determining stiffness coefficients, which are often subject to uncertainty. The method also demonstrates the

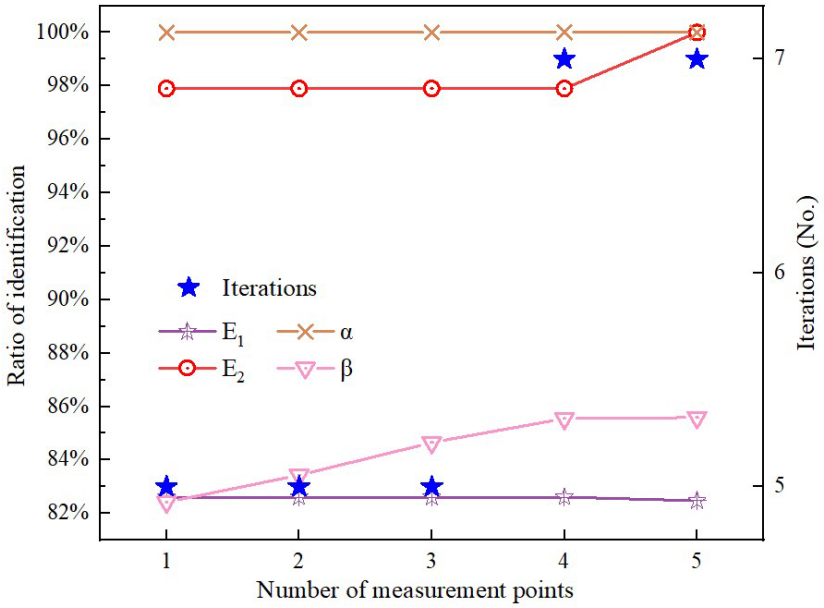

FIGURE 8. Inversion accuracy and iteration for different numbers of measurement points

advantage of rapidly converging to determine damping parameters. However, the influence of fractures and faults, as well as the heterogeneity and anisotropy of rock mass, are not considered. Although the continuum mechanics-based model provides a general framework for understanding rock behavior, it may not fully capture the nuances introduced by these geological complexities. Additionally, while the research discusses the impact of the number of measurement points on the identification process, the effect of relying solely on data from individual measurement points has not been thoroughly investigated.

5. **Conclusions.** A procedure is proposed for identifying the Rayleigh damping coefficients and elastic moduli of rock mass in the time domain. This procedure utilizes computed displacements derived from numerical finite element (FE) analysis, displacement sensitivity analysis, and the truncated singular value decomposition (TSVD) approach. The effectiveness of this method was validated through a sensitivity analysis using different initial system values, and the results indicated that the method exhibits high robustness against variations in initial seed values. Further confirmation was provided by Monte Carlo simulations and statistical analysis, demonstrating that the inversion results for rock mass mechanical parameters remain consistently stable and dependable, even in the presence of uncertainty associated with initial seed values.

The findings of this study highlight the potential for further research that could further refine the model by incorporating geological complexities such as fractures, faults, heterogeneity, and anisotropy. Incorporating these factors into the model can significantly enhance its predictive power and provide a more nuanced understanding of rock mass behavior. Additionally, future work should consider the impact of variability in data sources and the potential benefits of using data from multiple measurement points to ensure the accuracy and robustness of the identification process.

Acknowledgment. The authors gratefully acknowledge the financial support received from the State Key Laboratory of High Performance Civil Engineering Materials (in China), grant number 2022CEM006. We also sincerely acknowledge the funding provided

by a grant from the Utsunomiya City Hall and a donation from Chuden Engineering Consultants, Japan.

REFERENCES

[1] J. Stevenson, Structural damping values as a function of dynamic response stress and deformation levels, *Nuclear Engineering Design*, vol.60, no.2, pp.211-237, 1980.
[2] A. Fernández et al., Rock mass structural recognition from drill monitoring technology in underground mining using discontinuity index and machine learning techniques, *International Journal of Mining Science and Technology*, vol.33, no.5, pp.555-571, 2023.
[3] X. Gao et al., A geostatistical inverse approach to characterize the spatial distribution of deformability and shear strength of rock mass around an unlined rock cavern, *Engineering Geology*, vol.245, pp.106-119, 2018.
[4] T. Fei et al., Inversion analysis of rock mass permeability coefficient of dam engineering based on particle swarm optimization and support vector machine: A case study, *Measurement*, vol.221, 113580, 2023.
[5] M. Hasan et al., Determination of rock mass integrity coefficient using a non-invasive geophysical approach, *Journal of Rock Mechanics and Geotechnical Engineering*, vol.15, no.6, pp.1426-1440, 2023.
[6] M. Mirzaei, A. A. Moradi and M. Abbasi, Application of 2D inversion of apparent resistivity and RQD data in identification of granite massif quality, *Iranian Journal of Geophysics*, 2024.
[7] N. Yesiloglu-Gultekin and A. Dogan, Estimation of the elastic modulus of basaltic rocks using machine learning methods, *Earth Science Informatics*, pp.1-26, 2024.
[8] H. Wang et al., Determination of elastic modulus and anisotropy for rocks using digital drilling method, *Geoenergy Science Engineering Geology*, 213373, 2024.
[9] J. W. S. Rayleigh, *The Theory of Sound*, Macmillan, 1896.
[10] D. D'Angiò, L. Lenti and S. Martino, Microseismic monitoring to assess rock mass damaging through a novel damping ratio-based approach, *International Journal of Rock Mechanics and Mining Sciences*, vol.146, 104883, 2021.
[11] B. Yang et al., Experimental investigation and empirical model on damping properties of rock under multistage cyclic loading, *Soil Dynamics Earthquake Engineering and Engineering Dynamics*, vol.163, 107557, 2022.
[12] T. Arahira, M. Todo and A. Myoui, Fracture analysis of porous bioceramics by finite element method, *ICIC Express Letters, Part B: Applications*, vol.12, no.7, pp.619-625, 2021.
[13] B. R. Cox and D. P. Teague, Layering ratios: A systematic approach to the inversion of surface wave data in the absence of a priori information, *Geophysical Journal International*, vol.207, no.1, pp.422-438, 2016.
[14] B. Fennetteau et al., Update of Hoek and Marinos chart for predicting large deformation in tunnels, *New Challenges in Rock Mechanics and Rock Engineering*, pp.625-631, 2024.
[15] H. Li et al., Back analysis of geomechanical parameters for rock mass under complex geological conditions using a novel algorithm, *Tunnelling and Underground Space Technology*, vol.136, 105099, 2023.
[16] X. Chang, H. Wang and Y. Zhang, Back analysis of rock mass parameters in tunnel engineering using machine learning techniques, *Computers and Geotechnics*, vol.163, 105738, 2023.
[17] B. Liu et al., Prediction of rock mass parameters in the TBM tunnel based on BP neural network integrated simulated annealing algorithm, *Tunnelling and Underground Space Technology*, vol.95, 103103, 2020.
[18] J.-G. Be, Identification of viscous damping in structures from modal information, *Journal of Applied Mechanics*, vol.43, no.2, pp.335-339, 1976.
[19] J. N. Reddy, *An Introduction to the Finite Element Method*, McGraw-Hill, New York, 1993.
[20] K. Levenberg, A method for the solution of certain non-linear problems in least squares, *Quarterly of Applied Mathematics*, vol.2, no.2, pp.164-168, 1944.
[21] D. W. Marquardt, An algorithm for least-squares estimation of nonlinear parameters, *Journal of the Society for Industrial and Applied Mathematics*, vol.11, no.2, pp.431-441, 1963.
[22] J.-Y. Fan, A modified Levenberg-Marquardt algorithm for singular system of nonlinear equations, *Journal of Computational Mathematics*, pp.625-636, 2003.
[23] A. Fischer, A. F. Izmailov and M. V. Solodov, The Levenberg-Marquardt method: An overview of modern convergence theories and more, *Computational Optimization and Applications*, pp.1-35, 2024.

[24] K. Mishchenko, Regularized Newton method with global convergence, *SIAM Journal on Optimization*, vol.33, no.3, pp.1440-1462, 2023.
[25] W. Zhuang et al., Inversion analysis to determine the mechanical parameters of a high arch dam and its foundation based on an IAGA-BP algorithm, *Journal of Tsinghua University*, vol.62, no.8, pp.1302-1313, 2022.

Author Biography

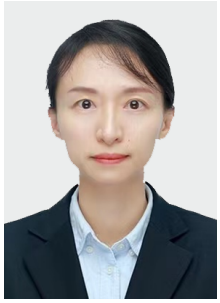

Rui Huang is an associate professor at Xihua University, China. She received her master degree in Civil Engineering from Xihua University in 2013, and is currently a Ph.D. candidate at Utsunomiya University, Japan. Her research interests include stability evaluation of underground spaces. She has published over 10 journal papers and is hosting some research projects funded from National Key Laboratory Foundation of China, etc.

Takafumi Seiki received the B.S. degree in Construction Engineering from Yamaguchi University, Ube, Japan in 1989, and M.S. degree in Civil Engineering, 1991 and Dr.Eng. in Geo Environmntal Engineering, 1994 in Nagoya University, Nagoya, Japan. Currently he is an associate professor at Department of Civil Engineering and Regional Design, Utsunomiya University, Utsunomiya, Japan. His research interests include rock weathering, rock cavern stability and underground space utilization.

Qinxi Dong is a professor at Hainan University, Ph.D. supervisor, Foreign Fellow of the Engineering Academy of Japan, Fellow of the Japan Society of Civil Engineers. He received his bachelor's degree in Solid Mechanics from the School of Aerospace at Beijing Institute of Technology in 1986, a master's degree in Computational Mechanics from the same university in 1989, and a Ph.D. degree in Science and Technology in Computational Mechanics from the University of Innsbruck in Austria in 1997. From 1998 to 2000, he conducted postdoctoral research at the Japan Society for the Promotion of Science (JSPS). His research interests include high-performance computing and supercomputing algorithms, with applications in seismic engineering, intelligent manufacturing and carbon-neutral technologies.

Satoshi Yamaoka received his Master Engineering degree in Tokyo Institute of Technology, Japan, in 1985, and the Ph.D. degree in Ritsumeikan University, Japan, in 2012. He is currently a professor at Ustunomiya University, where his research interests include electric power development engineering, dam engineering, water resources engineering, water supply technology and project management.

Ömer Aydan obtained his B.Sc. degree in Mining Engineering from Istanbul Technical University, Turkey, in 1979 and M.Sc. degree in Rock Mechanics and Excavation Engineering from University of Newcastle Upon Tyne in 1982, and his Ph.D. degree in Rock Mechanics from Nagoya University, Japan, in 1989. He worked at Nagoya University as a research associate (1987-1991), and at the Department of Marine Civil Engineering at Tokai University, first as assistant professor (1991-1993), then as associate professor (1993-2001), and finally as professor (2001-2010). He then became professor of the Institute of Oceanic Research and Development at Tokai University. He moved to University of the Ryukyus in Nov. 2013 as a professor at the Department of Civil Engineering, Nishihara, Okinawa, Japan and retired in March 2020 as an emeritus professor. He was the member of the organizing committee of EUROCK2016. He received the 2005 technology award, the 2012 Frontier award and the 2015 Best Paper award of Japan Society of Rock Mechanics (JSRM), the excellent contributions award of the International Association for Computer Methods and Advances in Geomechanics (IACMAG), as well as the 1998 Matsumae Technology award of Tokai University and the 2018 Excellent Research Contribution award of University of the Ryukyus and the 2018 best paper award of Active Fault Society of Japan. He has published 8 books as a part of ISRM Book Series by CRC Press. He has been elected as "ISRM Vice-President at Large" on Sep. 2019 in 14th Congress of iSRM held in Iguassu, Brazil. He was also made Honorary Professor in Earth Science by Pamukkale University (Denizli, Turkey) in 2008. His research interests include rock stability assessment under dynamic conditions, covering rock mechanics, excavation engineering, and geohazard mitigation.